Int. J. Heat Mass Transfer. Vol. 12, pp. 935–951. Pergamon Press 1969. Printed in Great Britain

THE INFLUENCE OF FOREIGN GAS INJECTION AND SLOT GEOMETRY ON FILM COOLING EFFECTIVENESS

W. K. BURNS and J. L. STOLLERY

Department of Aeronautics, Imperial College of Science and Technology, London, England

(*Received* 10 *October* 1968, *and in revised form* 12 *February* 1969)

Abstract—Measurements of foreign gas concentration are presented for a wide range of velocity and density ratios. The mainstream boundary layer thickness and slot lip geometry were varied in order to investigate the importance of these parameters through the range of velocity and density ratios covered.

The value of mass concentration at the wall increased continuously with mass flux injected, though the improvement was relatively small for velocity ratios greater than unity.

For a given mass flux of foreign gas the wall value of *mass*-concentration (and hence by analogy the adiabatic wall film cooling effectiveness based on enthalpy) was slightly greater for the lightest gas injected. The corresponding wall value of *mole*-fraction (analogous to effectiveness based on adiabatic wall *temperature*) was considerably greater for the lightest gas.

Increasing the slot lip thickness lowered the film cooling effectiveness and its influence increased as the coolant density was reduced. The effect of increasing the mainstream boundary layer thickness was much smaller though still significant when a light gas coolant was used.

The present results are compared with other experimental data and with the predictions of the boundary layer model of film cooling flows.

NOMENCLATURE

C, mass fraction of foreign gas in mixture of foreign gas and air;
C_p, specific heat at constant pressure;
h_0, stagnation enthalpy;
K, volumetric concentration (mole-fraction) of foreign gas in mixture of foreign gas and air;
k, a constant;
m, mass-velocity ratio, $\rho_c u_c/\rho_m u_m$;
M, molecular weight;
p, pressure;
Re, Reynolds number;
s, slot height;
t, thickness of slot upper lip;
T, temperature;
u, velocity;
$\hat{u}$, maximum velocity;
x, streamwise distance;
$\bar{x}$, boundary layer correlation parameter $\dfrac{x}{ms}\left[Re_c\dfrac{\mu_c}{\mu_m}\right]^{-0.25}$;
y, distance normal to free-stream direction.

Greek symbols

δ, 90% boundary layer thickness;
η' impervious wall effectiveness $(C_w - C_m)/(C_c - C_m)$ or adiabatic wall effectiveness $(h_{aw} - h_{om})/(h_{oc} - h_{om})$;
η'' impervious wall effectiveness $(K_w - K_m)/(K_c - K_m)$ or adiabatic wall effectiveness $(T_{aw} - T_{om})/(T_{oc} - T_{om})$;
μ, viscosity;
ρ, density.

Subscripts

aw, adiabatic wall;
c, slot;
m, mainstream;
w, wall.

1. INTRODUCTION

THE USEFULNESS of film-cooling for the alleviation of surface heating is well established. The most common applications of the technique are the protection of combustion chambers and tail pipes in gas turbine engines. Film cooling is sometimes used to protect exhaust nozzles in rocket motors and may be needed to alleviate the severe kinetic heating effects suffered by hypervelocity vehicles.

The possibility of using fuel or foreign gas as a coolant has led to considerable research into heterogeneous film cooling flows [1, 2]. Even when the coolant and mainstream gases are the same it is often easier experimentally to study the effects of density gradients due to temperature differences by using a foreign gas under isothermal conditions and invoking Reynolds' Analogy (with the implicit assumption of unit turbulent Lewis Number). Thus, impervious wall effectiveness data for heterogeneous mixing experiments, such as those presented here, may be used to predict the analogous adiabatic wall conditions needed for practical design.

The aims of the present work are two-fold, (i) to provide new experimental data for comparison with both theory and previous experiments, (ii) to draw attention to the importance of lip geometry and initial flow conditions in the subsequent mixing process.

By using mixtures of Arcton-12† with air, and helium with air, a wide range of mass-velocity ratios ($0{\cdot}07 \leqslant m \leqslant 16{\cdot}7$) have been covered. Injection to mainstream density ratios in the range $0{\cdot}14 \leqslant \rho_c/\rho_m \leqslant 4{\cdot}17$ have been used at a nominal velocity ratio of unity. Further tests were conducted with velocity ratios in the range $0{\cdot}53 \leqslant u_c/u_m \leqslant 4{\cdot}0$ for the two extreme density ratios of 0·14 and 4·17.

Two different thicknesses of mainstream boundary-layer and two widely different lip thicknesses have been tested to assess the sensitivity of effectiveness measurements to these variables.

Impervious wall effectiveness has been deduced from the observed variation of mass-fraction of foreign gas along the wall. If the turbulent Lewis Number is unity then this is analogous to the adiabatic wall effectiveness based on enthalpy in the true film-cooling situation. Experimental data for values of the turbulent Lewis Number are sparse. Zakkay, Krause and Woo [3] measured the turbulent Lewis Number for the turbulent free mixing of coaxial gas streams of helium, hydrogen and argon. The values obtained lay between 0·3 and 1·2. Their measurements also suggested that the Lewis Number varied considerably with mixture concentration and this fact casts doubts on the validity of invoking the mass to heat transfer analogy even for comparative purposes. However, the most relevant comment is implicit in the experimental data of Goldstein, Rask and Eckert [1] which showed the very close agreement between mass-transfer measurements in film-cooling experiments using pure helium as the coolant in an air mainstream. Comparisons are made here with the adiabatic wall measurements of Goldstein *et al.* [1] and Hatch and Papell [2] and with the wall concentration measurements of Goldstein *et al.* [1] and Pai and Whitelaw [6]. Data from all the above sources are compared with the predictions of the boundary layer model [7, 8].

2. DESCRIPTION OF APPARATUS

The Aeronautics Department 18 × 18 in. closed working section open return low-speed wind tunnel is shown in Fig. 1. It is a "blowing" tunnel with centrifugal fan driven by a synchronous motor. The working section airspeed is varied by changing pulley sizes on the toothed belt drive system. Air is taken in through a filter box from the laboratory. After passing through the working section the airstream takes a 90° turn through corner vanes and exhausts through the laboratory window to atmosphere. The

† Arcton-12 is a trade name for dichlorodifluoromethane C Cl_2F_2 or Freon-12.

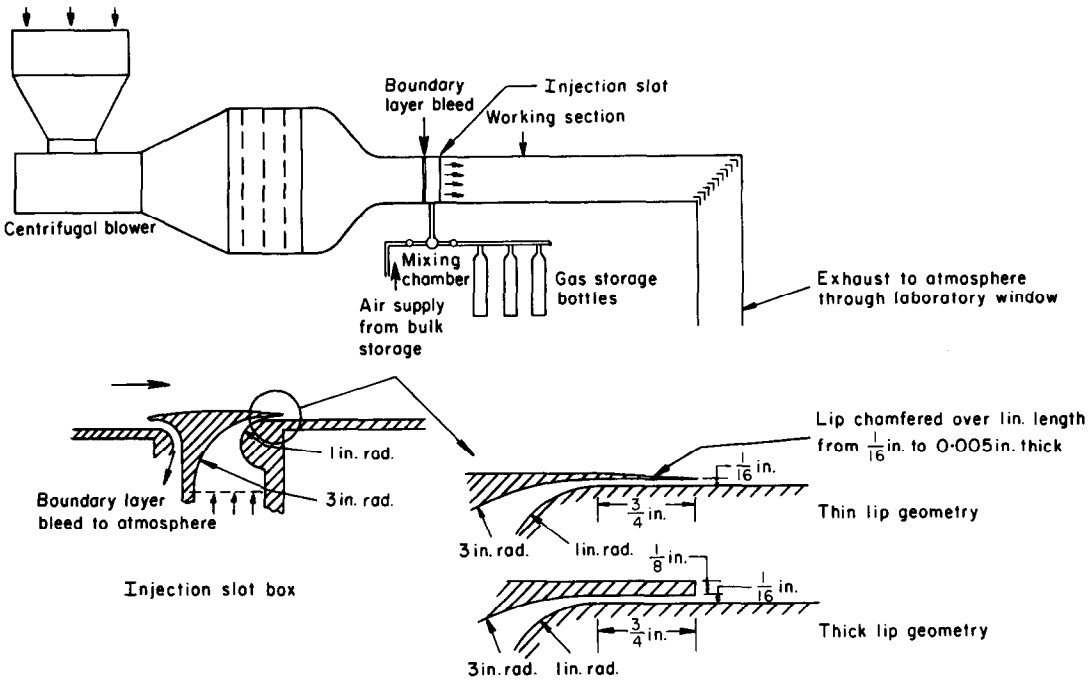

FIG. 1. Layout of 18 in. wind tunnel, test-plate and slot geometry.

working section operates at a pressure slightly above atmospheric pressure due to the small pressure drop through the corner vanes.

The working section has been designed for versatility of use in film-cooling work. It has an easily removable injection slot assembly which exhausts the injected stream tangentially along a removable floor of dural plate.

The plate has a series of 0·025 in. dia. holes which can be used for withdrawing samples or measuring wall static pressure. The plate rests on three jacking screws so that its angle may be adjusted through a limited range in order to achieve zero pressure gradient conditions.

The roof of the working section is made up of removable shutters, one of which carried the traversing gear. The shutters are constructed in various sizes chosen to facilitate location of the traversing gear in any position throughout the 6 ft length of the working section.

The injection slot box (Fig. 1) is constructed of Paxolin† and rests on locating flanges bolted to the working section sub-frame. The internal contraction is of moulded Araldite and in the present work had a contraction ratio of 48:1. The upper lip of the slot is formed by a $\frac{1}{16}$ in. thick gauge plate chamfered over a 1 in. length on its top surface to 0·005 in. at slot exit. For some runs this was replaced by a square edged plate of $\frac{1}{8}$ in. thickness behind which there must inevitably be some base flow but which may be more representative of practical slot design.

The tunnel boundary layer is completely removed through a bleed duct (Fig. 1) but a new boundary layer grows over the 6 in. "starting length" ahead of the injection slot. The "starting

† A plastic manufactured by Micanite and Insulators Co. Ltd.

length" boundary layer could be artificially thickened by adding roughness or a trip wire.

The air supply for injection through the slot is provided by the department's high-pressure bulk air storage system. The supply line was throttled before passing to a manifold which also received lines from either three helium cylinders or three Arcton-12 cylinders. The air supply line and foreign gas lines could be throttled independently to provide a "tailored" mixture at the injection slot.

Profiles of velocity and mass-fraction are obtained using a motorised traversing system. Continuous output of dynamic pressure during a traverse is achieved using a pressure transducer so close to the probe that its response time is short enough to prevent profile distortion at a useful traversing speed.

The traverse drive is a reversible 12 V d.c. motor which drives both the traverse lead-screw and a helical potentiometer. The potentiometer gives an output voltage which is a linear function of probe position to within 0·01 per cent of its full scale output.

Dynamic head profiles were obtained using an I.R.D. micromanometer† with, in the present experiments, a transducer whose sensitivity was 250 mV/in. water gauge with a linearity within 2 per cent of full scale output. This was calibrated before and after each run against an inclined single leg manometer. The transducer was connected to the probe by about 12 in. of tubing and this was found to yield a tolerable response time.

The total head probe had a flattened orifice whose frontal dimensions were:

internal: 0·003 × 0·032 in.
external: 0·020 × 0·050 in.

Output voltages from the helical potentiometer (proportional to probe position) and from the transducer (proportional to $\frac{1}{2}\rho u^2$) were fed via a control panel to a Mosely $X-Y$ recorder‡ whose sensitivity and linearity were sufficiently good to render any errors at this stage of signal processing negligible relative to those at the transducing stage.

Analysis of gas-mixture constituents on a continuous basis has been achieved using a microkatharometer† of the through-flow type with the heated wires directly in the sample stream. This, together with a total passage volume of only 2·6 μl, enables a short response time to be achieved which would not be possible with the more conventional diffusion type katharometer where the heated wires are in a side passage and dependent upon relatively slow molecular diffusion from the sample stream. Unfortunately, however, the through flow katharometer is very sensitive to flow rate and it is therefore important to ensure that the pressure drop across the cell is constant during sampling. The design philosophy of this type of katharometer is outlined in [9].

The cell was calibrated for mixtures of Arcton-12 in air and for mixtures of helium in air by injecting mixtures of known composition using a constant, known cell pressure drop and pressure within the cell. The calibration mixtures were made up in a 100 ml syringe. The calibrations obtained were valid for the cell during subsequent operation provided that the cell pressure drop and cell pressure were the same as those used for the calibration.

The total probable uncertainty in mole fraction measurements amounts to not more than 2·5 per cent of full scale and arises from the cumulative effects of drift in bridge supply voltage, drift in cell pressure drop and uncertainty in calibration.

The calibrations and analysis were carried out with a cell pressure drop of 8 in. alcohol and vacuum of 19·5 in. alcohol upstream of the cell. These figures were arrived at as a compromise between the need for a short response time (governed by the travelling time of a slug of sampled gas from the probe to the cell)

† Hilger-I.R.D. Ltd., 98 St. Pancras Way, Camden Road, London, N.W.1.

‡ Hewlett Packard, Mosely Division, California.

† Developed by the Distiller's Company, Ltd. and marketed by Servomex Controls of Crowborough, Sussex.

and the desirability of sampling sub-isokinetically so that the samples were representative of the smallest possible diameter stream-tube in the boundary layer. Constituent separation at the probe by baro-diffusion is quite negligible at the flow velocities used in the present work.

The sampling conditions used yielded a response time of 0·5 sec and a sampling velocity at the probe tip of about 42 ft/s (48 ml/min). The traversing speed was kept at speeds sufficiently low to eliminate the risk of concentration profile distortion due to the 0·5 second response time of the cell. However, if higher traversing speeds are desirable correction for the finite response time simply involves an axis shift on the trace.

As with the dynamic head profiles the concentration profiles were plotted on the X–Y recorder.

3. THE EXPERIMENTS

As a preliminary to the main experimental programme a zero pressure gradient boundary layer flow was set up so that velocity profiles could be compared with the universal turbulent velocity profile. The floor plate was raised on jacking-screws so that it was flush with the square, $\frac{1}{8}$ in. thick upper lip of the injection slot, thus producing a flat plate with boundary layer bleed at its rounded leading edge. A 3 in. roughness strip was located near the leading edge to ensure a fully turbulent profile. Velocity profiles were recorded at a distance of 41·5 in. from the leading edge of the plate for a free stream velocity of 56·2 ft.s^{-1}.

With the film cooling geometry restored, two dimensionality checks of $\frac{1}{2}\rho u^2$ and mole-fraction at the slot exit and far downstream were carried out.

For the effectiveness measurements two series of runs were performed. Table 1 outlines the conditions of runs 1–17 in which the thin lip geometry was used. The effect of velocity ratio $\hat{u}_c/u_m$ on effectiveness was observed at density ratios ρ_c/ρ_m of 4·17 (Arcton-12 into air) and $\rho_c/\rho_m = 0{\cdot}14$ (helium into air). The velocity ratios were in the range $0{\cdot}53 \leqslant \hat{u}_c/u_m \leqslant 4{\cdot}0$ and two values of u_m were used. Table 2, covering runs 20–33, outlines a series of runs at a nominal velocity ratio of unity, i.e. a peak slot velocity to free-stream velocity $\hat{u}_c/u_m$ of unity. Two different mainstream boundary layer thicknesses on the slot upper lip and two slot lip geometries were used in this series of runs. Six density ratios were achieved by tailoring an injection mixture from Arcton-12 and air for $\rho_c/\rho_m > 1$ and from helium and air for $\rho_c/\rho_m < 1$.

Table 1. Runs with 100 per cent Arcton-12 injection or 100 per cent helium injection at $0{\cdot}50 < \hat{u}_c/u_m \leqslant 4{\cdot}0$. Thin, chamfered slot lip

	Run No.	$\hat{u}_c/u_m$	u_m(ft.s^{-1})
	1	0·58	19·8
	2	0·93	19·8
	3	1·15	19·8
100 per cent	4	2·00	19·8
Arcton-12 Injection	5	3·00	19·8
	6	4·00	19·8
$\frac{\rho_c}{\rho_m} = 4{\cdot}17$	7	0·53	57·0
	8	0·77	57·0
	9	1·01	57·0
	10	1·18	57·0
	11	1·40	57·0
	12	1·60	57·0
100 per cent helium	13	0·51	55·0
Injection	14	0·81	55·0
	15	1·03	55·0
$\frac{\rho_c}{\rho_m} = 0{\cdot}14$	16	1·36	55·0
	17	1·68	55·0

Table 2. Runs with injection of Arcton-12/air mixture or helium/air mixtures at a nominal velocity ratio of unity and density ratios within the range $0{\cdot}14 \leqslant \rho_c/\rho_m \leqslant 4{\cdot}17$

	Thick mainstream boundary layer, $\delta/s = 2{\cdot}54$		Thin mainstream boundary layer, $\delta/s = 0{\cdot}90$	
ρ_c/ρ_m	thin lip	thick lip	thin lip	
4·17	20	24	28	run No.
2·50			29	
1·38	21	25		
1·09			31	
0·60	22	26		
0·30	23			
0·14	33	27	32	

For each of the 31 runs profiles of $\frac{1}{2}\rho u^2$ and mole fraction were recorded at (usually) eight streamwise stations within the range $0 < x/s \leqslant 512$. The profiles produced on the X–Y recorder were converted into digital form on a D-MAC cartographic digitiser and subsequently reduced by computer.

4. PRESENTATION AND DISCUSSION OF RESULTS

4.1 *Comparisons with the universal turbulent-velocity profile*

The velocity profiles measured in the zero-pressure gradient boundary layer flow without injection were used to construct a Clauser plot [10] and hence to calculate the skin-friction coefficient at $x = 41{\cdot}5$ in. A value of 0·0033 was obtained. This compares favourably with the value of 0·0036 predicted from the formula due to Schultz–Grunow [11] which assumes a fully turbulent boundary layer growing from the leading edge of a flat plate with zero pressure-gradient. The comparison encourages confidence in the measured velocity profiles.

4.2 *Two dimensionality of the film-cooling flow*

Checks on the two-dimensionality of the flow were made at $x/s = 0$, 100 and 256. Profiles of $\frac{1}{2}\rho u^2$ and mass concentration were measured at 15 spanwise stations located at 1 in. intervals across the plate.

At $x/s = 0$ the scatter on measured upper-lip boundary layer thickness was less than $\pm 2\frac{1}{2}$ per cent of the mean. Scatter on velocity measurements in the slot was less than ± 1 per cent of mean. Mixture composition within the slot was uniform to within ± 1 per cent of the mean mass-fraction of foreign gas and at $x/s = 256$ the scatter was ± 3 per cent.

At $x/s = 100$ the scatter on velocity measurements was ± 3 per cent of free-stream velocity and at $x/s = 256$ this had increased to ± 6 per cent within 3 in. on either side of the centre line. In all cases the scatter was random and not systematic in the spanwise direction.

4.3 *Conservation of foreign gas*

A check on the integrated flux of foreign-gas in the boundary layer is a sensitive test of two-dimensionality and repeatability of injection conditions. Such a check was made at eight streamwise stations and the observed scatter on integrated species-flux was typically about 12 per cent. This large degree of scatter in the integral check arose from the superposition of

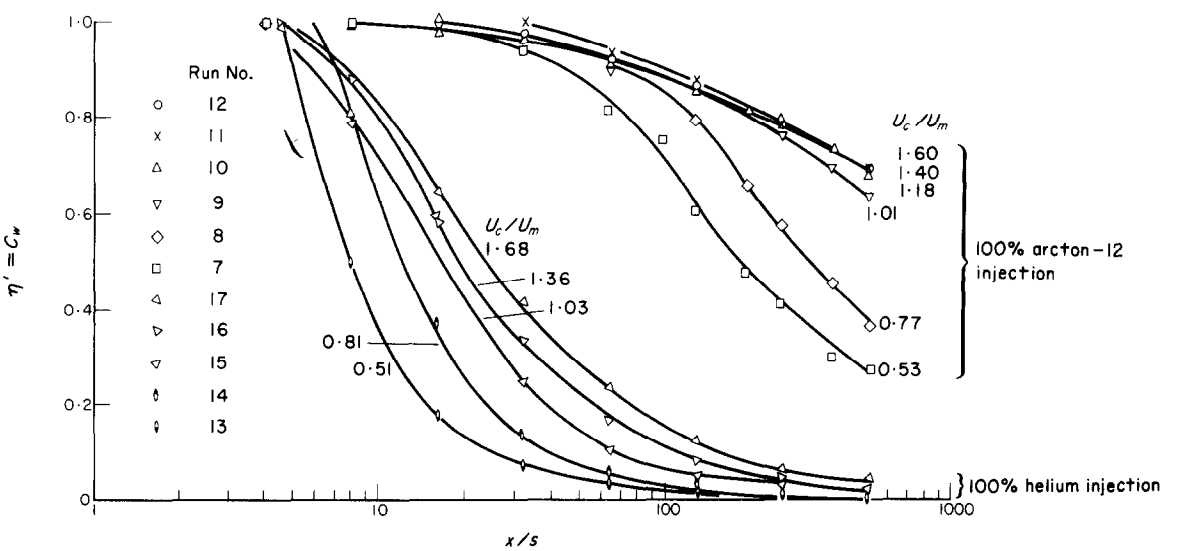

FIG. 2. Effect of coolant jet velocity ratio for the extreme density ratios.

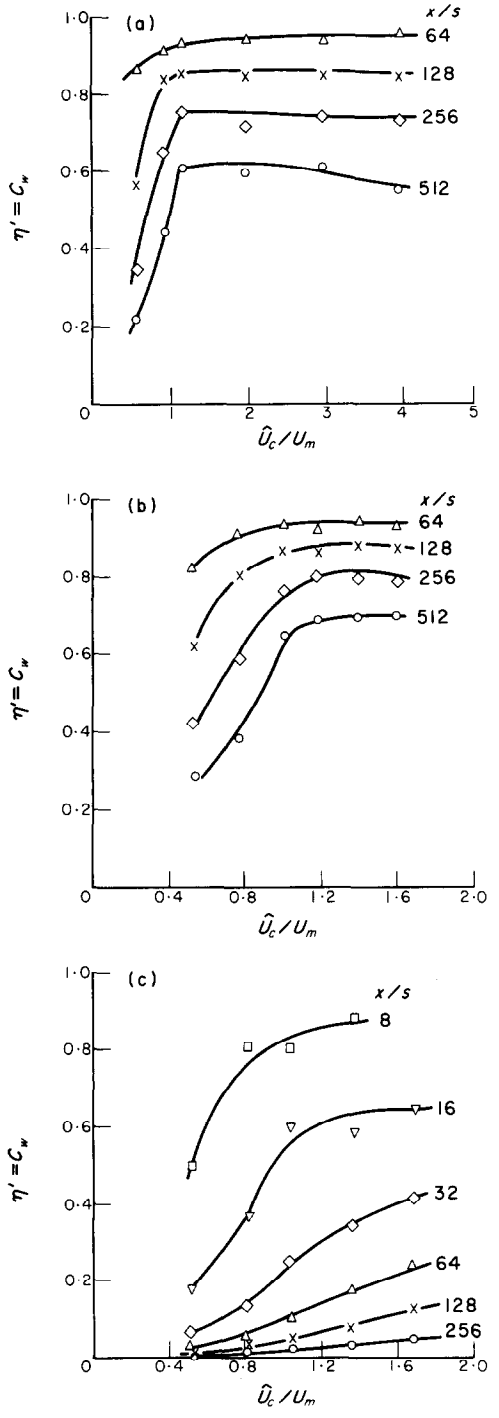

FIG. 3. The effect of coolant jet velocity ratio (a) Arcton-12 injection; u_m = 19·8 ft/s; (b) Arcton-12 injection; u_m = 57 ft/s; (c) helium injection u_m = 55 ft/s.

individual errors in the components of the product ρuC making up the integral.

Measurements of mass-fraction, however, are accurate to within about 4 per cent of unity and yield effectiveness measurements to within 8 per cent when the injected gas is a two-component mixture.

4.4 *Impervious wall effectiveness measurements*

Figure 2 shows a semi-logarithmic plot of effectiveness against x/s over the range $0{\cdot}5 < u_c/u_m < 1{\cdot}7$ for 100 per cent Arcton-12 injection and 100 per cent helium injection using the thin lip geometry. For all the runs presented in Fig. 2 the mainstream velocity (u_m) was about 57 ft/s (see Table 1). The figure clearly shows the superior protection afforded by the largest mass flux of injected fluid.

For Arcton-12 at velocity ratios greater than unity the curves tend to crowd into each other. Figures 3(a), (b) and (c) show cross-plots of

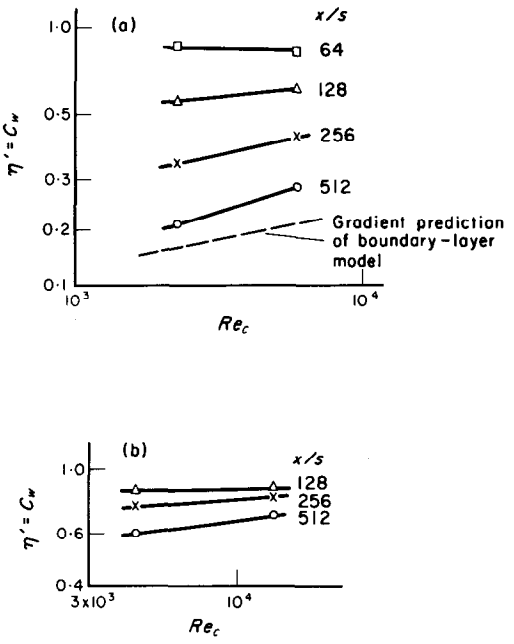

FIG. 4. Variation of effectiveness with slot Reynolds number for Arcton-12 injection (a) $\frac{\hat{u}_c}{u_m} = 0{\cdot}53$; (b) $\frac{\hat{u}_c}{u_m} = 1{\cdot}15$.

η' against $\hat{u}_c/u_m$ for runs 1–17. Figures 3(a) and 3(b) show the variation of η' with $\hat{u}_c/u_m$ for Arcton-12 injection. In both figures the effectiveness approaches the maximum close to a velocity ratio of unity and incremental improvements in effectiveness for $\hat{u}_c/u_m$ rising above unity are very small. In contrast Fig. 3(c) shows the variation of η' with $\hat{u}_c/u_m$ for helium injection where η' continues to rise with $\hat{u}_c/u_m$ even for $\hat{u}_c/u_m \gg 1$.

Comparing Fig. 3(a) and 3(b) we see indications of the influence of slot Reynolds number. The higher absolute velocities of Fig. 3(b) yield higher values of η' for a given $\hat{u}_c/u_m$. The simple boundary layer model (7) of the film cooling situation predicts a slot Reynolds number dependence $\eta' \alpha [Re_c]^{0.2}$ and some of the data of runs 1–12 have been plotted in Fig. 4 to indicate the Reynolds number dependence shown by the present results. It seems from Fig. 4 that Reynolds number dependence becomes more significant as x/s increases and as $\hat{u}_c/u_m$ decreases, i.e. the very régimes where the boundary layer model is most plausible. The effect of Re_c at $x/s \leqslant 64$ appears to be very small.

Figure 5(a) shows the variation of η' against x/s for the density ratio range $0{\cdot}14 \leqslant \rho_c/\rho_m \leqslant 4{\cdot}17$ and nominal unit velocity ratio. The results are for the thin lip geometry. Figure 5(b) shows a cross-plot of the same data against ρ_c/ρ_m, the data points being interpolated from Fig. 5(a).

The superior protection afforded by higher values of mass flux is again demonstrated. However, for the range of x/s of practical interest in many film cooling situations ($x/s < 50$) indications of "saturation" are apparent, i.e. incremental improvements in effectiveness for a given x/s become smaller with increasing ρ_c/ρ_m.

Figure 6 presents comparisons of effectiveness obtained with the two slot geometries for unit velocity ratio and $\rho_c/\rho_m = 0{\cdot}14$, 1·38 and 4·17.

The consequences of an injection geometry with high drag caused by wake flows behind areas of large material thickness are already known to be serious. Kacker and Whitelaw [12] and Sivasegaram and Whitelaw [13] have reported data from geometries with large lip-thickness to slot-height ratios. Price [14] and Holland [15] have presented results from more practical geometries with three-dimensional irregularities which also reduce the effectiveness.

Our results show that these effects are more pronounced for low values of ρ_c/ρ_m. For example, Fig. 6 shows a 50 per cent reduction in the local value of η' for $10 \leqslant x/s \leqslant 100$ when $\rho_c/\rho_m = 0{\cdot}14$ but the reduction drops to only 10 per cent when $\rho_c/\rho_m = 4{\cdot}17$.

The effects of a thick slot lip are strikingly demonstrated by the velocity and concentration profiles for helium injection (Fig. 7). Increasing the lip thickness draws the helium jet into the base flow and causes a separation bubble on the plate below. Thus at $x/s = 4$ the velocity profile indicates a reversed flow region whilst the concentration profile shows that the maximum value is no longer at the wall. A sketch of the flow, since confirmed by schlieren pictures is included in Fig. 7.

Similar observations of separation bubbles in wake regions with small amounts of base bleed have been reported for co-axial free-jet configurations by Ferri [16], Fox, Zakkay and Sinha [17] and by Williams and Grey [18].

In contrast the influence of the slot lip on Arcton-12 flow is quite small (Fig. 8). The larger wake from the thick lip is quickly absorbed and by $x/s = 16$ the profiles are somewhat similar to those obtained using a thin lip.

Figure 9 shows three comparisons between runs performed with two different mainstream boundary layer thicknesses, $\delta/s = 0{\cdot}90$ and 2·54. Again the velocity ratio was unity with density ratios of 4·17, 1·38 and 0·14. There appears to be little effect of mainstream boundary layer in the downstream region where the assumptions of the boundary layer model are valid.

Nearer the slot the effects of changing the boundary layer thickness are more marked. It is expected that increasing δ would enhance mixing and lower the value of η' near the slot. This is indeed the trend shown by the tests made

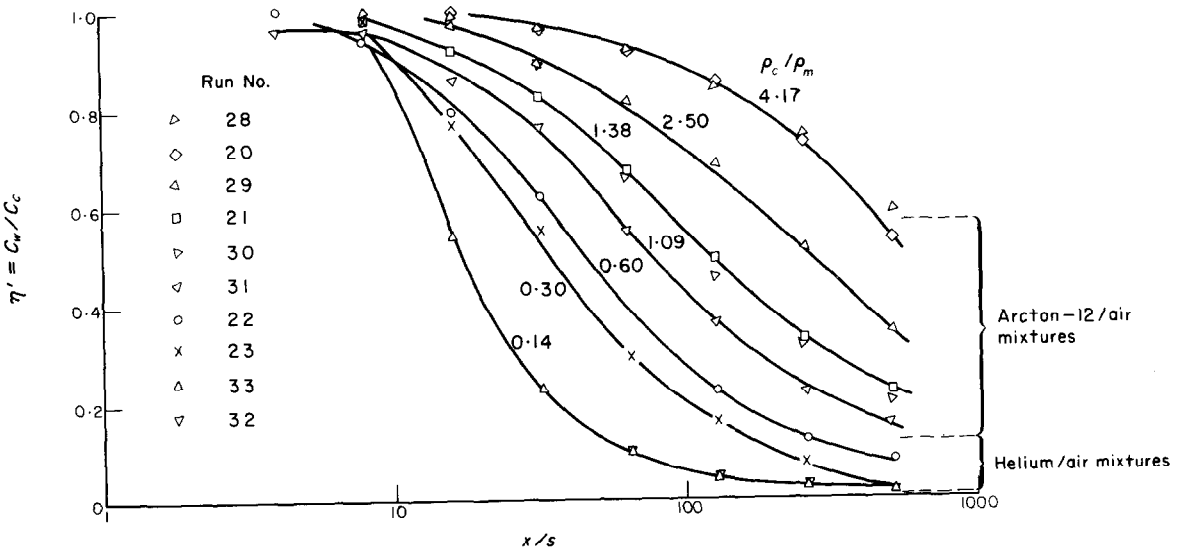

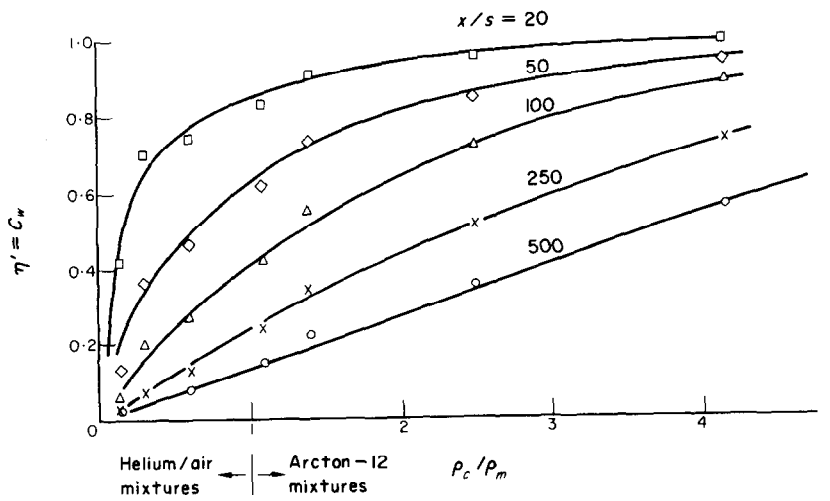

FIG. 5. Effect of coolant jet density ratio at $\hat{u}_c/u_m \simeq 1$: thin lip geometry.

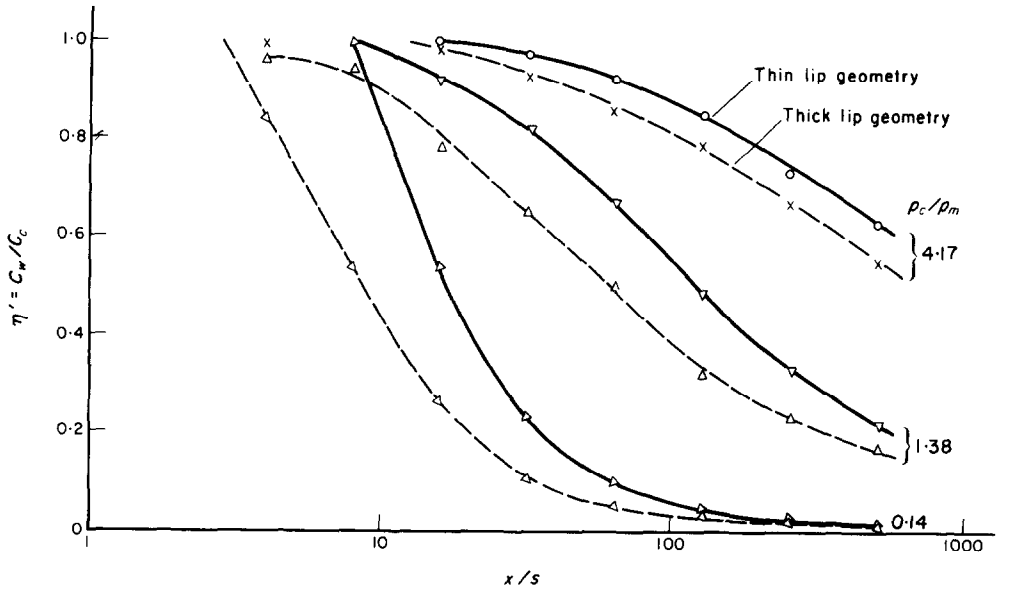

FIG. 6. Effect of injection slot geometry at $\hat{u}_c/u_m \doteq 1$.

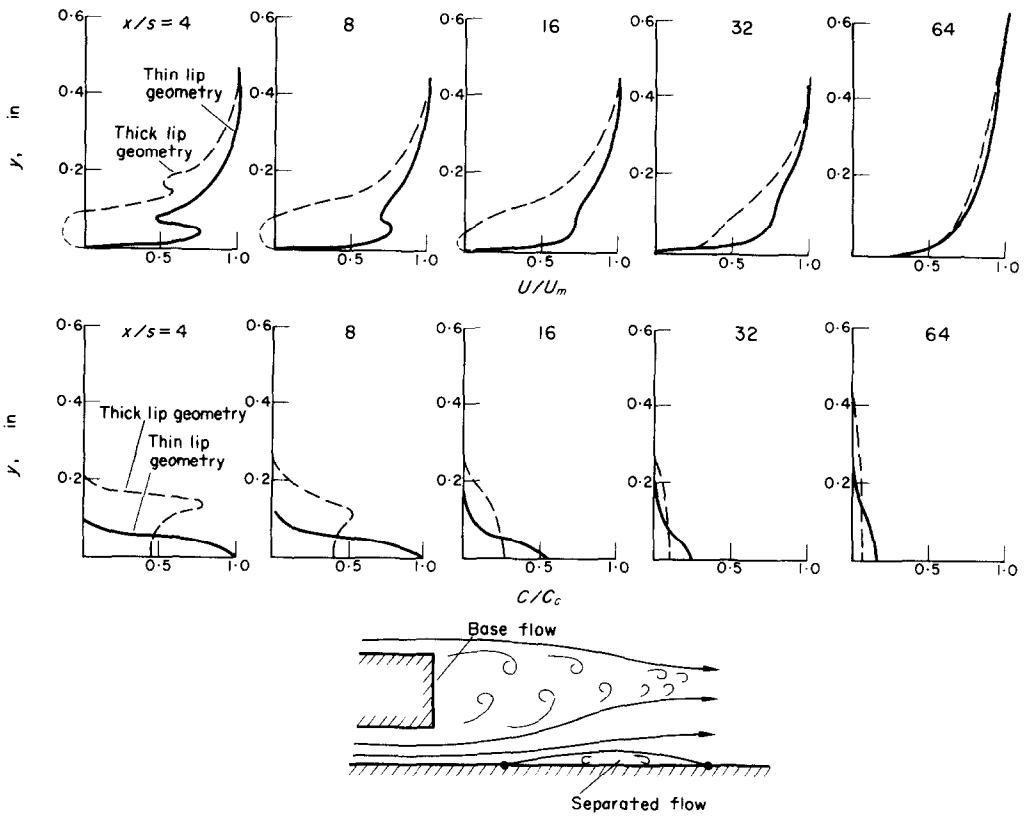

FIG. 7. Effect of slot geometry on velocity and mass-fraction profiles: 100 per cent helium injected into air, $\hat{u}_c/u_m \doteq 1$.

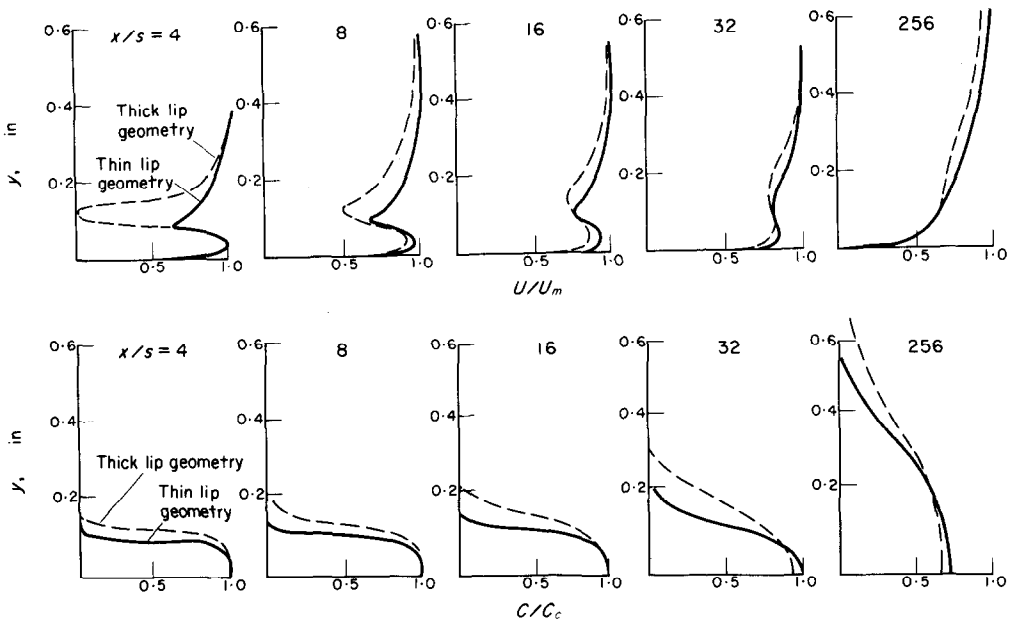

FIG. 8. Effect of slot geometry on velocity and mass-fraction profiles: 100 per cent Arcton-12 injected into air; $\hat{u}_c/u_m \simeq 1$.

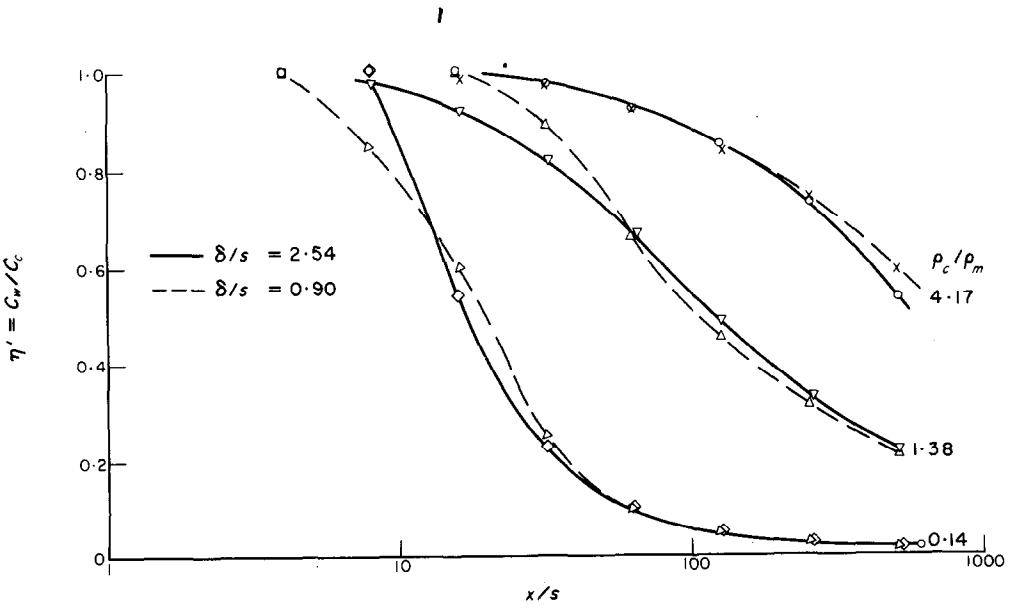

FIG. 9. Effect of mainstream boundary layer thickness; $\hat{u}_c/u_m \simeq 1$ clean slot geometry.

with $\rho_c/\rho_m = 1{\cdot}38$. It might further be argued that the mainstream boundary layer contributes to the overall momentum deficit at $x/s = 0$ which arises from both the slot and mainstream boundary layers together with any base drag from the slot lip. The effect of changing δ would then be expected to decrease as the coolant density was increased, as demonstrated by the results with $\rho_c/\rho_m = 4{\cdot}17$. The anomalous result using helium as the coolant may be connected with the transition from laminar to turbulent flow which took place a few slot widths downstream of the injection plane for all helium injection runs.

The conclusions are in qualitative agreement with those of Kacker and Whitelaw [4] and Seban [5] and extend their conclusions to flows with large density ratios.

5. COMPARISONS WITH OTHER EXPERIMENTAL DATA AND THE PREDICTIONS OF THE BOUNDARY LAYER MODEL

Semi-empirical correlations based on a boundary layer model of film cooling flows have been widely used with varying degrees of success. Most of the experimental data have been obtained using similar gases for both coolant and mainstream flows and very few data are available where density gradients due to both temperature and concentration were present. It is therefore worth reviewing the data where large density differences are present, no matter from what source, and comparing them with the data presented here and the predictions of the boundary layer model.

Stollery and El-Ehwany [7] reviewed the origins, development and utility of the boundary layer model and concluded that a correlation equation of the type

$$\eta' = \frac{h_{aw} - h_{om}}{h_{oc} - h_{om}} = A\left\{\frac{x}{ms}\left[Re_c\frac{\mu_c}{\mu_m}\right]^{-\frac{1}{4}}\right\}^{-0{\cdot}8} = \{\bar{x}\}^{-0{\cdot}8} \qquad (1)$$

is useful for all density ratios provided $u_c/u_m <$ 1·5. They also showed [8] that the corresponding analogous expression for mass concentration at the wall is given by

$$\eta' = \frac{C_w - C_m}{C_c - C_m} = B\{\bar{x}\}^{-0{\cdot}8}. \qquad (2)$$

If a pure gas is injected then $C_m = 0$, $C_c = 1$ and $\eta' = C_w$. The constants A and B depend on the assumptions made concerning the shape and growth of the velocity, temperature and concentration profiles. A and B are numerically similar though not necessarily the same. They depend critically on initial flow conditions but are typically between 3 and 5 for "clean" slot geometries.

Often it is preferred to express film cooling effectiveness in terms of total temperature in which case it can be shown that [7]

$$\eta'' = \frac{T_{aw} - T_{om}}{T_{oc} - T_{om}} = \frac{\alpha}{(\alpha - 1) + 1/\eta'} \qquad (3)$$

where

$$\alpha = C_{p_c}/C_{p_m}.$$

The analogous expression for concentration by volume is

$$\eta'' = \frac{K_w - K_m}{K_c - K_m} = \frac{\gamma}{(\gamma - 1) + 1/\eta'}. \qquad (4)$$

where $\gamma = M_c/M_m$.
For a pure gas $K_m = 0$, $K_c = 1$ and $\eta'' = K_w$.

In a recent paper Goldstein *et al.* [1] give both the wall concentration by volume (K_w) and the film cooling effectiveness η''. They show that both sets of data are well correlated by plotting against $\bar{x}$. The "best lines" which they fit to their data have been converted to lines of C_w and η' using equations (3) and (4) used in the figures discussed below.

Figure 10 compares our measurements of C_w for pure helium injected into an air mainstream with those of Goldstein *et al.* The scatter is considerable in both sets of data and their data lies somewhat below our own as expected since they used a porous strip instead of a discrete

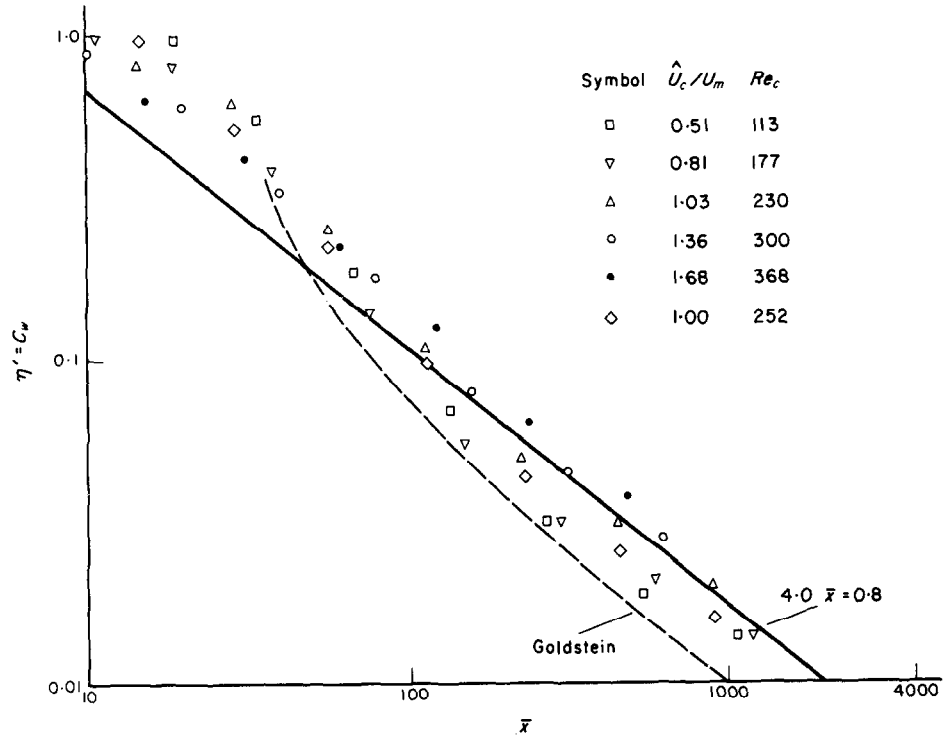

FIG. 10. Pure helium injection, wall concentration measurements: a comparison with the data of Goldstein *et al.* [1].

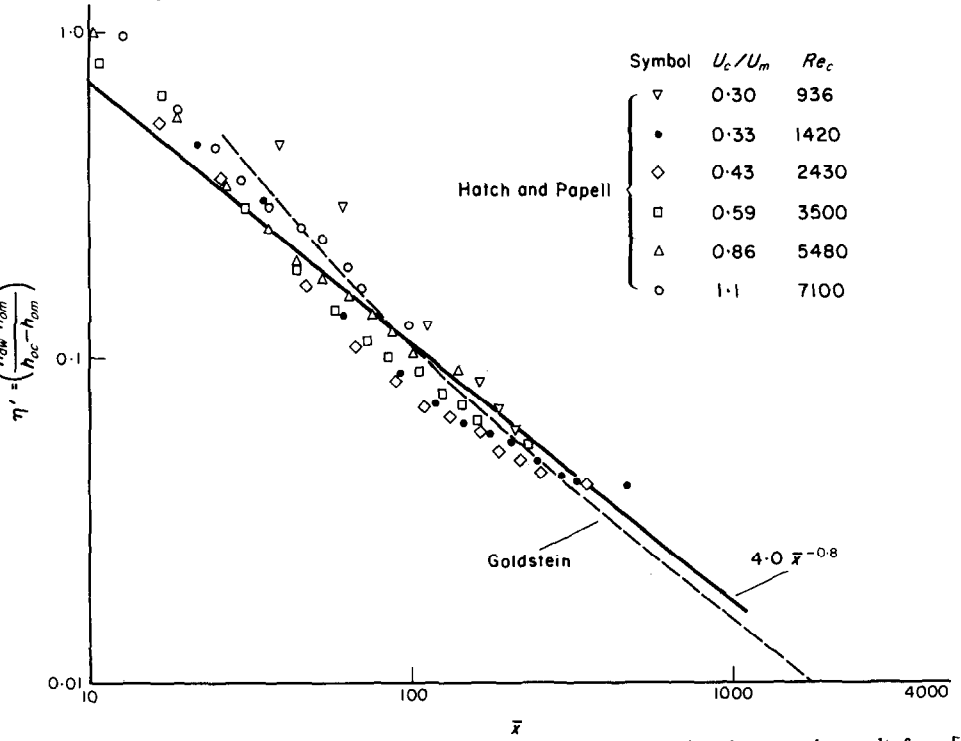

FIG. 11. Pure helium injection, adiabatic wall temperature measurements: a comparison between the results from [1] and [2].

slot for injection. The trends, however, are identical: the wall concentration asymptotes to a line $k\bar{x}^{-0.8}$ far downstream but it asymptotes to the lines from above. This is in contrast to the air and heavy gas injection results displayed in Fig. 13.

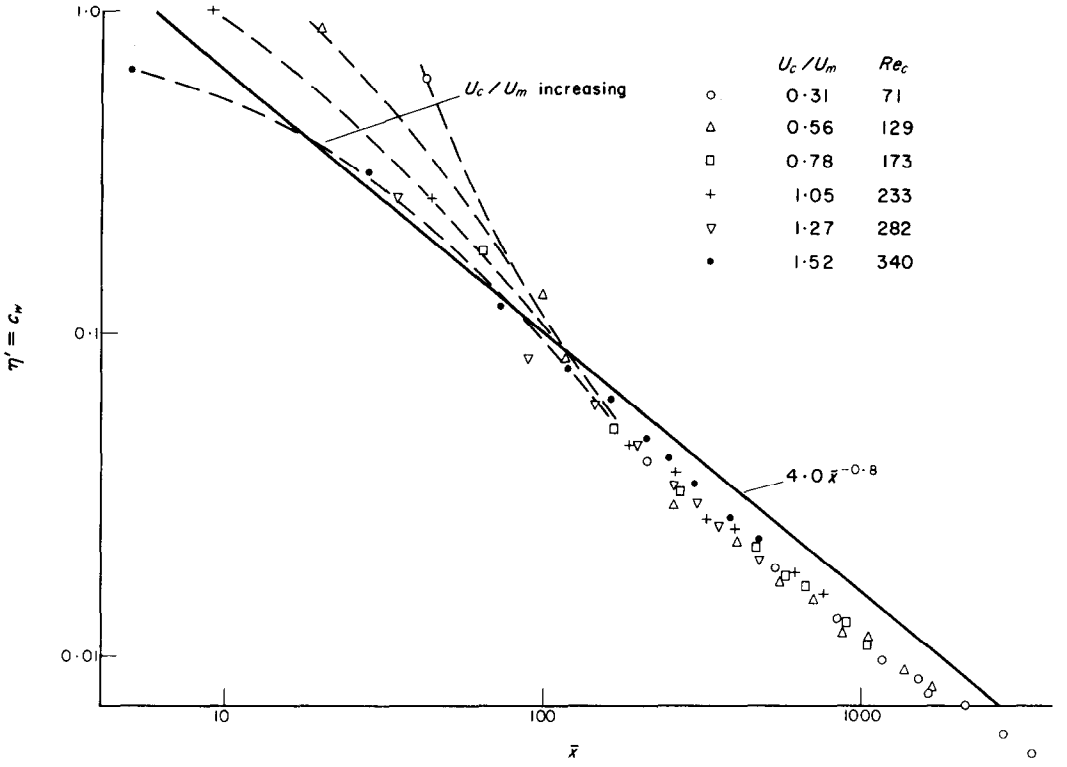

FIG. 12. Pure hydrogen injection; data of Pai and Whitelaw [6].

The trends of Fig. 10 are again exhibited in Fig. 11 where the film cooling effectiveness measurements of Goldstein are compared with some of those taken by Hatch and Papell [2]. To complete the survey of light gas injection data, Fig. 12 shows how well the hydrogen injection measurements of Pai and Whitelaw correlate according to the boundary layer model except near the slot exit. In all the figures the line C_w or $\eta' = 4\bar{x}^{-0.8}$ is plotted to facilitate comparison between the separate graphs.

It is noticeable in Fig. 12 that as the coolant velocity increases so the data come more into line with the prediction of the turbulent boundary layer theory. The associated slot Reynolds numbers are so low that the jet is laminar and transition occurs a few slot widths downstream of the slot exit.

The same trend is again evident in Fig. 13 which collects together all our thin lip geometry data. No matter whether the slot Reynolds number is increased by raising U_c or ρ_c the effect is the same, the effectiveness is lowered for small x/s and the data asymptotes more rapidly to the line $\eta' = 4\bar{x}^{-0.8}$.

Tabulated data for the results reported here may be found in [19].

6. CONCLUSIONS

With pure Arcton-12 as "coolant" increasing

the velocity ratio $\hat{u}_c/u_m$ produces higher effectiveness values though for $\hat{u}_c/u_m > 1$ the improvements in effectiveness are small. In contrast, for pure helium injection the effectiveness continues to improve with rising $\hat{u}_c/u_m$ even when $\hat{u}_c/u_m \gg 1$.

For large x/s the slot Reynolds number influence is in reasonable agreement with the predictions of the boundary layer model i.e. $\eta' \alpha Re_c^{\frac{1}{2}}$ but for small x/s the slot Reynolds number influence is small.

For values of x/s less than about 100 predictions of the boundary layer model are unreliable, particularly for values of $\rho_c \rho_m$ very much less than unity. This is due in part to

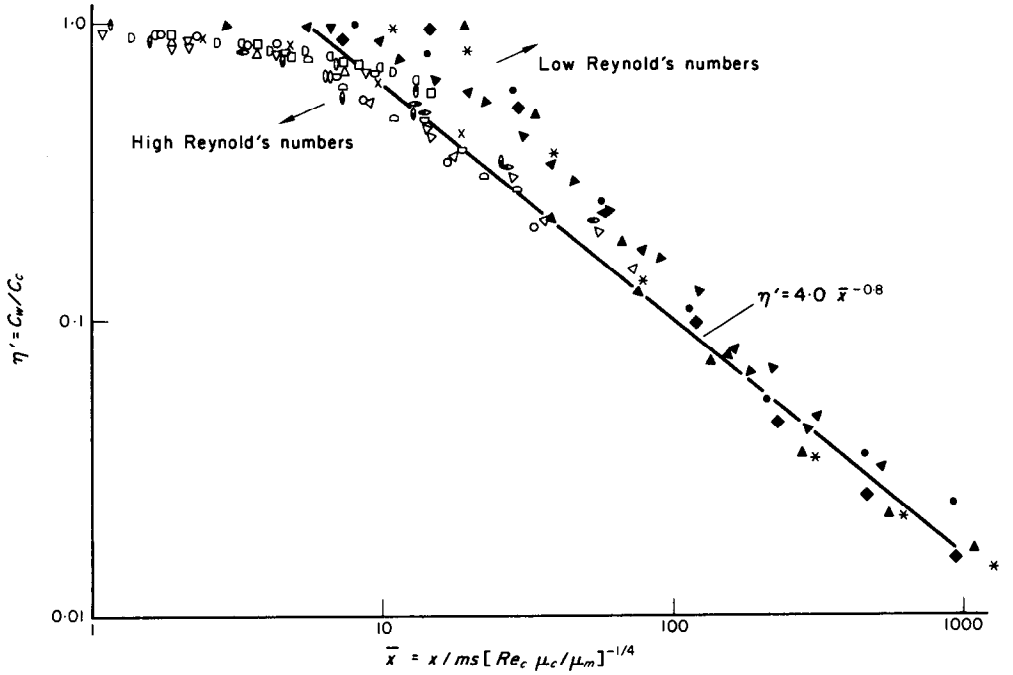

Arcton-12 and Arcton-12/air mixtures

Symbol	Run No.	U_c/U_m	ρ_c/ρ_m	Re_c	m
⊷	20	1·0	4·17	11300	4·17
⊷	21	1·0	1·38	2720	1·38
⊷	28	1·0	4·17	10100	4·17
⊷	29	1·0	2·50	4680	2·50
▷	30	1·0	1·38	2190	1·38
◁	31	1·0	1·09	1784	1·09
○	1	0·58	4·17	2220	2·42
×	2	0·93	4·17	3560	3·88
□	3	1·51	4·17	4390	6·30
◇	4	2·00	4·17	7550	8·33
△	12	1·60	4·17	17450	6·67
▽	11	1·40	4·17	15460	5·84
D	10	1·18	4·17	13100	4·91
◻	9	1·01	4·17	11200	4·21
◻	8	0·77	4·17	8460	3·21
◻	7	0·53	4·17	5850	2·21

Helium and helium/air mixtures

Symbol	Run No.	U_c/U_m	ρ_c/ρ_m	Re_c	m
◆	33	1·00	0·14	228	0·14
▶	23	1·00	0·30	481	0·30
◀	22	1·00	0·60	970	0·60
•	15	1·03	0·14	230	0·144
*	14	0·81	0·14	177	0·114
▲	13	0·51	0·14	113	0·071
▶	17	1·68	0·14	368	0·236
◀	16	1·36	0·14	300	0·191

FIG. 13. Present data; thin slot geometry.

laminar flow at the slot for the low density ratio tests reported here.

The consequence of thickening the slot lip is a decrease in effectiveness. This effect is particularly serious for low values of ρ_c/ρ_m.

The influence of mainstream boundary layer thickness on effectiveness is, in general, small. However, there is evidence suggesting it can become important if ρ_c/ρ_m is low; presumably since the momentum deficit in the boundary layer in these circumstances is of the same order of magnitude as the momentum of the injectant.

For a given mass flow of injectant issuing from a thin lipped slot the highest mole-fraction (temperature effectiveness) values were achieved using the lightest gas (pure helium).

REFERENCES

1. R. J. GOLDSTEIN, R. B. RASK and E. R. G. ECKERT, Film-cooling with helium injection into an incompressible air flow. *Int. J. Heat Mass Transfer*, **9**, 1–10 (1966).
2. J. E. HATCH and S. S. PAPELL, Use of a theoretical model to correlate data for film cooling or heating an adiabatic wall by tangential injection of gases of different fluid properties. NASA TN D-130, 1959.
3. V. ZAKKAY, E. KRAUSE and S. D. L. WOO, Turbulent transport properties for axisymmetric heterogeneous mixing. *AIAA Jl.* **2**, No. 11. 1939–1947 (1964).
4. S. C. KACKER and J. H. WHITELAW, The dependence of the impervious wall effectiveness of a two dimensional wall-jet on the thickness of the upper-lip boundary layer. *Int. J. Heat Mass Transfer* **10**, 1623–1624 (1967).
5. R. A. SEBAN, Effects of initial boundary layer thickness on a tangential injection system. *J. Heat Transfer* **82**, 392–393 (1960).
6. B. R. PAI and J. H. WHITELAW, The influence of density gradients on the effectiveness of film-cooling. British Aeronautical Research Council, Current Paper No. 1013 (1968).
7. J. L. STOLLERY and A. A. M. EL-EHWANY, A note on the use of a boundary layer model for correlating film cooling data, *Int. J. Heat Mass Transfer* **8**, 55–65 (1965).
8. J. L. STOLLERY and A. A. M. EL-EHWANY, Shorter communication on above, *Int. J. Heat Mass Transfer*, **10**, 101–105 (1967).
9. G. PREAU and G. GUICHON, Rapid analysis by gas-chromatography V, A katharometer with rapid response, *J. Gas Chromatogr.* **4**, 343–346 (1966).
10. F. H. CLAUSER, Turbulent boundary layers in adverse pressure gradients, *J. Aero. Sci.* **21**, 91–108 (1954).
11. F. SCHULTZ-GRUNOW, NACA TM 986, 1941.
12. S. C. KACKER and J. H. WHITELAW, The effect of slot height and slot turbulence intensity on the effectiveness of the uniform density, two-dimensional wall jet, *J. Heat Transfer* **90(C)**, 469–475 (1968).
13. S. SIVASEGARAM and J. H. WHITELAW, Film cooling slots: the important of lip thickness and injection angle, *J. Mech. Engng Sci.* **11**, 22–27 (1969).
14. R. B. PRICE, Summary of cooling tests on a film-cooled parallel duct. Bristol Siddeley Engines Ltd., APRG Report A.P. 5312 (1965).
15. M. J. HOLLAND, Film cooling in air breathing engines. Bristol Siddeley Engines Ltd., AP 5338 (1965).
16. A. FERRI, A critical review of heterogeneous mixing problems, *Astronautica Acta* **13**, 453–465 (1968).
17. H. FOX, V. ZAKKAY and R. SINHA, A review of some problems in turbulent mixing. New York Univ. AA-66-63 Sept. (1966).
18. P. M. WILLIAMS and J. GREY, Simulation of gaseous core nuclear rocket mixing characteristics using cold and arc-heated flows. NASA CR-690 (1967).
19. W. K. BURNS and J. L. STOLLERY, Film cooling: the influence of foreign gas injection and slot geometry on impervious wall effectiveness. Imperial College Aero Dept. Report EHT/TN/12. (1968).

Résumé—On présente des mesures de concentration de gaz étranger pour une large gamme de rapports de vitesses et de masses volumiques. L'épaisseur de la couche limite de l'écoulement principal et la géometrie de la lèvre de la fente ont été modifiées de façon à étudier l'importance de ces paramètres dans la gamme étudiée des rapports de vitesses et de masses volumiques. La valeur de la concentration massique à la paroi augmentait continûment avec le flux massique injecté, bien que l'amélioration ait été relativement faible pour des rapports de vitesses plus grands que l'unité.

Pour un flux massique donné de gaz étranger, la valeur pariétale de la concentration *massique* (et, par analogie, l'efficacité de refroidissement de film pariétal adiabatique basée sur l'enthalpie' était légèrement plus grande pour le gaz le plus léger injecté. La valeur pariétale correspondante de la fraction *molaire* (analogue à l'efficacité basée sur la *température* pariétale adiabatique) était considérablement plus grande pour le gaz le plus léger.

En augmentant l'épaisseur de la lèvre de la fente, l'efficacité de refroidissement de film est abaissée et son influence augmentée lorsque la densité du réfrigérant était réduite. L'effet d'augmenter l'épaisseur de la couche limite de l'écoulement principal était beaucoup plus faible bien qu'encore sensible lorsqu'on employait un réfrigérant gazeux léger.

Les résultats actuels sont comparés avec d'autres données expérimentales et avec les prévisions du modèle du type couche limite pour les écoulements de refroidissement par film.

Zusammenfassung—Es werden Messungen der Fremdgaskonzentration über einen weiten Bereich der Geschwindigkeits- und Dichteverhältnisse widergegeben. Dabei wurde die Dicke der Hauptstromgrenzschicht und die Geometrie des Schlitzes verändert, um den Einfluss dieser Parameter in dem untersuchten Bereich der Geschwindigkeits- und Dichteverhältnisse zu ermitteln. Der Wert der Massenkonzentration an der Wand wächst stetig mit dem zugeführten Massenstrom, obwohl die Verbesserung ziemlich gering ist für Geschwindigkeitsverhältnisse grösser als Eins.

Für einen gegebenen Massenstrom des Fremdgases ist der Wert der Massenkonzentration an der Wand (und somit analog die von der Enthalpie abgeleitete Wirksamkeit der adiabaten Wandkühlung durch einen Fluid-Film) etwas grösser für das leichteste eingeblasene Gas. Der entsprechende Wert des Molenbruches an der Wand (analog zur adiabaten Wandtemperatur) ist beachtlich grösser für das leichteste Gas.

Mit wachsender Dicke des Ausblaseschlitzes nimmt die Wirksamkeit der Filmkühlung ab, und zwar wächst dieser Einfluss mit abnehmender Dichte des Kühlgases. Die Auswirkungen einer zunehmenden Dicke der Hauptstromgrenzschicht sind viel geringer, allerdings noch deutlich spürbar, wenn ein leichtes Kühlgas benützt wird.

Die vorliegenden Ergebnisse werden mit anderen experimentellen Daten und mit den auf Grund des Grenzschichtmodells für Filmkühlung gewonnenen Voraussagen verglichen.

Аннотация—Представлены результаты измерения концентрации инородного газа в широком диапазоне изменений скорости и плотности. Толщина пограничного слоя основного потока и геометрия щели изменялись с целью исследования значения этих параметров в рассматриваемом диапазоне отношений скорости и плотности. Величины концентрации массы на стенке возрастали с повышением плотности вдуваемого потока массы, хотя для отношения скоростей больше единицы достигаемое при этом увеличение было незначительным. Для данного потока массы инородного компонента величина концентрации массы у стенки (и, следовательно, эффективность адиабатического пленочного охлаждения стенки, отнесенная к энтальпии) была немногим больше при вдувании самых легких газов. Соответствующее пристеночное значение молярной концентрации (аналогично эффективности, отнесенной к температуре адиабатическои стенки) было значительно выше для самых легких газов. При увеличении высоты щели снижалась эффективность пленчного охлаждения; влияние этой высоты увеличивалось при уменьшении плотности охладителя. При использовании легкого охладителя влияние роста толщины пограничного слоя основного потока было гораздо менее заметным, хотя и достаточно значительным.

Результаты данной работы сравниваются с другими экспериментальными данными и с расчетами пограничного слоя при пленочном охлаждении.